

2102Ep embryonal carcinoma cells have compromised respiration and shifted bioenergetic profile distinct from H9 human embryonic stem cells

Authors: Lyudmila Ounpuu¹, Aleksandr Klepinin¹, Martin Pook², Indrek Teino², Nadezda Peet³, Kalju Paju³, Kersti Tepp¹, Vladimir Chekulayev¹, Igor Shevchuk¹, Sulev Koks², Toivo Maimets², and Tuuli Kaambre^{4,1*}

¹Laboratory of Bioenergetics, National Institute of Chemical Physics and Biophysics, Akadeemia tee 23, 12618 Tallinn, Estonia.

²Department of Cell Biology, Institute of Molecular and Cell Biology, University of Tartu, Riia 23, 51010 Tartu, Estonia.

³Institute of Biomedicine and Translational Medicine, University of Tartu, Ravila 19, 50411 Tartu, Estonia.

⁴Tallinn University, Narva mnt 25, 10120 Tallinn, Estonia.

*Corresponding author: TuuliKaambre, Laboratory of Bioenergetics, National Institute of Chemical Physics and Biophysics, Akadeemia tee 23, 12618 Tallinn, Estonia; e-mail address: tuuli.kaambre@kbfi.ee; tel. +372 6398381.

Abstract

Recent studies have shown that cellular bioenergetics may be involved in stem cell differentiation. Considering that during cancerogenesis cells acquire numerous properties of stem cells or dedifferentiate, it is possible to assume that the energy metabolism in tumorigenic cells might be differently regulated. The aim of this study was to compare the mitochondrial bioenergetic profile of normal pluripotent human embryonic stem cells (hESC) and relatively nullipotent embryonal carcinoma cells (2102Ep cell line).

We examined three parameters related to cellular bioenergetics: phosphotransfer system, aerobic glycolysis, and oxygen consumption. Activities and expression levels of main enzymes that facilitate energy transfer were measured. The oxygen consumption rate studies were performed to investigate the respiratory capacity of cells. In addition, we applied

Abbreviations:

ADP, adenosine diphosphate; **AK**, Adenylate kinase; **ANT**, adenine nucleotide translocator; **ATP**, adenosine triphosphate; **BSA**, bovine serum albumin; **CAT**, carboxyatractyloside; **CK**, creatin kinase; **CKB**, brain-type creatine kinase; **CKMT1A**, creatine kinase, mitochondrial 1A; **CKMT2**, creatine kinase, mitochondrial 2; **CS**, citrate synthase; **CSC**, cancer stem cells; **Cyt c**, Cytochrome c; **ETC**, electron transport chain; **FBS**, fetal bovine serum; **FCC**, flux control coefficient; **FCCP**, Carbonyl cyanide 4-(trifluoromethoxy)phenylhydrazone; **hESCs**, human embryonic stem cells; **HK**, hexokinase; **hMSCs**, human mesenchymal stem cells; **MCA**, metabolic control analysis; **NEM**, N-ethylmaleimide; **OCR**, oxygen consumption rate; **OXPHOS**, oxidative phosphorylation; **RCI**, Respiratory control index; **RCR**, respiratory control ratio; **ROS**, reactive oxygen species; **ROX**, residual oxygen consumption; **TCA cycle**, tricarboxylic acid cycle; **TMPD**, N,N,N',N'-tetramethyl-p-phenylenediamine; **VDAC**, voltage dependent anion channel.

metabolic control analysis to identify target reactions that control oxygen consumption in both cell lines.

2102Ep cells showed a shift in energy distribution towards adenylate kinase network. The total AK activity was almost 3 times higher in 2102Ep cells compared to hESCs (179.85 ± 5.73 vs 64.39 ± 2.55 mU/mg of protein) and the expression of AK2 was significantly higher in these cells, while CK was downregulated. 2102Ep cells displayed reduced levels of oxygen consumption and increased levels of aerobic glycolysis compared to hESCs. The compromised respiration of 2102Ep cells is not the result of increased mitochondrial mass, increased proton leak, and reduced respiratory reserve capacity of the cells or impairment of respiratory chain complexes. We also noted that the respiration chain might be distinctly organized in studied cell lines since FCC values for complexes II and IV, ATP synthase and ANT were considerably higher in 2102Ep cells than in hESCs that value in hESCs.

Our data showed that the bioenergetic profile of 2102Ep cells clearly distinguishes them from normal hESCs. This should be considered when this cell line is used as a reference, and highlight the importance of further research concerning energy metabolism of stem cells.

Keywords: Embryonal carcinoma, human embryonic stem cells, cellular bioenergetics

Highlights:

- bioenergetic profile of 2102Ep embryonal carcinoma cells clearly distinguishes them from normal hESCs
- 2102Ep cells have elevated levels of adenylate kinase 2 and reduced levels of creatine kinase compared with hESCs
- 2102Ep cells display reduced levels of OXPHOS and elevated levels of aerobic glycolysis
- respiration chain is distinctly regulated in 2102Ep cells compared with normal hESCs

1 Introduction

There are increasing evidences that cancer could be considered as a stem cell disease [1]. As aging induces mutations in stem cells [1], it supports the idea of cancer stem cells (CSCs) evolving from different stem cell compartments. CSC has been defined as “a cell within a tumor that possesses the capacity to self-renew and to cause the heterogeneous lineages of cancer cells that comprise the tumor”[2]. It has been demonstrated that CSCs are involved in cancer onset and development, distant metastasis, angiogenesis and drug resistance [3]. The development of specific strategies to eradicate highly malignant CSCs holds a great potential for cancer treatment [4-5]. In light of novel observations on how core metabolic properties of CSCs might contribute to tumor progression and resistance to conventional treatment, the

cellular metabolism of CSCs may represent an attractive target for cancer therapy. However, these therapies may cause toxicity to normal stem cells, which share many common features with CSCs [6]. In order to develop safe and effective cancer therapy, it is crucial to understand shared and distinguishing mechanisms that regulate proliferation in normal and cancer stem cells.

The bioenergetic profiles of various human progenitor and stem cells are just being understood. It is clear now, that energy metabolism plays an important role in the homeostasis and differentiation of stem cells. Differentiation of the cell is accompanied by changes in mitochondrial metabolism, activity and organization of electron transport chain (ETC) complexes [7-9]. Moreover, recent studies have demonstrated that mitochondrial metabolism itself can influence the stemness maintenance and differentiation process [9-10]. Although stem cells contain fewer number and morphologically more immature mitochondria than differentiated cells[9], the ETC complexes within the inner membrane of the mitochondria are functionally active and mitochondria are able to consume oxygen and produce ATP from oxidative phosphorylation (OXPHOS)[10-11].

The reprogramming of energy metabolism is proposed as one of the hallmarks of cancer[12]. It has been shown that cancer cells are able to modulate their energy metabolism via aerobic glycolysis[13]. This inclination of cancer cells to use glycolysis even in the presence of oxygen characterizes also normal stem cells[14]. One of the mechanisms that explain high glycolytic rate in tumor cells at normoxic condition is Warburg-Pedersen model[15]where the association between glycolytic enzyme hexokinase (HK) and mitochondrial outer membrane enhances aerobic glycolysis in cancer cells. It has been demonstrated that HK bound to voltage dependent anion channel (VDAC) utilizes ATP produced during OXPHOS to catalyze the first reaction of glycolysis[15]. A similar mechanism may occur in stem cells, which also overexpress HK enzymes[10].

Well-organized high-energy phosphoryl transfer system is required to mediate intracellular communication between ATP-consuming and ATP-producing cellular compartments and thus maintain normal growth and development of cell [16].The main components of phosphotransfer system are adenylate kinase (AK) network, creatine kinase (CK) network and glycolysis[16]. CK network maintains normal phosphate levels in cells with high energy demands. Mitochondrial CK isoforms, CKMT1A and CKMT2, as well as cytosolic isoform, CKB, provide energy for various cellular processes[16]. AK1, the major cytosolic isoform, and AK2, localized in mitochondrial intermembrane space, have been recognized as the main

facilitators of intracellular nucleotide exchange in cells with compromised CK network. AK4, enzymatically inactive isoform, has been proposed as a marker of poor clinical outcome for lung cancer [17].

Recent studies have shown that adenylate kinase and creatine kinase networks are involved in the differentiation of hematopoietic stem cells facilitating energy transfer and metabolic signaling required for developmental programming [18-19]. The cancerogenesis has been also associated with the reorganization of the phosphotransfer system. The creatine kinase system is significantly downregulated in various cancer types including breast cancer [20], Ehrlich ascites carcinoma [21], neuroblastoma [22], colorectal cancer [23] and prostate cancer [24]. On the contrary, AK levels were found to be elevated in several types of cancer [22-23]. However, the exact role of CK and AK enzymes in the regulation of cell stemness or cancer development remains elusive.

In the present study, we used 2102Ep cell line derived from a primary human testicular teratocarcinoma [25] as a CSC model. Described as relatively nullipotent, this cell line has been shown to express many of the identified markers of pluripotent hESCs [26], as well as, numerous oncogenes and has many potentially tumorigenic genomic alterations [27]. Embryonic stem cell-like gene expression signature has been found to be characteristic of poorly differentiated aggressive tumors [28-29]. With limited differentiation potential 2102Ep resembles these undifferentiated cancer cells that are often associated with poor prognosis of cancer patients. Embryonic stem cells represent the normal counterparts of embryonal carcinoma cells and together, these can be used as complementary tools for studying pluripotency, stem cell biology and cancer [30]. We examined differences between normal human embryonic stem cells and 2102Ep cells in the three parameters related to cellular bioenergetics: phosphotransfer system, aerobic glycolysis, and oxygen consumption. In addition, we applied the metabolic control analysis to compare the effect of inhibition of different respiratory complexes on the respiratory efficiency in the two cell lines.

2 Material and methods

2.1 Cell cultures

2.1.1 2102Ep cell line

The human embryonal carcinoma cell line 2102Ep(Cl.2/A6; GlobalStem) was routinely cultured in T75 (Greiner bio-one) flasks in high glucose Dulbecco's modified Eagle medium with L-glutamine, supplemented with 10% heat inactivated fetal bovine serum (FBS), penicillin (100 U/ml), streptomycin (100 µg/ml) and 50 µg/ml gentamicin. Cells were grown at high density to limit spontaneous differentiation [31] and maintained at 37°C in a humidified incubator containing 5% CO₂ in the air.

2.1.2 H9 cell line

Pluripotent H9 human embryonic stem cells (WA09, National Stem Cell Bank, WiCell) were cultured on 6-well tissue culture plates (BD Biosciences) coated with Matrigel (BD Biosciences) in mTeSR1 media (STEMCELL Technologies) according to the manufacturer's specifications. The culture medium was changed daily. Cells were passaged mechanically with micropipette tip after 3-4 days and cultured in the presence of 5% CO₂ at 37°C in humid conditions. Normal karyotype of the cells was confirmed by G-banding.

2.1.3 Oxygen consumption rate (OCR) study

The rates of oxygen consumption were measured at 25°C using an Oxygraph-2k (Oroboros Instruments, Innsbruck, Austria). Measurements were performed in Mitomedium B solution supplemented with 5mM glutamate, 2mM malate and 1mg/ml BSA. A suspension of cells (1×10^6 cells/ml) was placed in the oxygraph chamber, permeabilized with saponin (40µg/ml) and allowed to equilibrate for 5 min. 10mM succinate was added to initiate electron transport through Complex II. State 2 respiration was monitored and after that 2 mM ADP was added to evaluate state 3 respiration. Respiration rates were normalized to the total protein amount in the cells and expressed as nmol of O₂ consumed per /min/per mg of total protein (nmol/(min x mg)). Protein concentrations were determined using the Pierce BCA Protein Assay Kit.

The functional coupling between HK and mitochondria was measured as described earlier. [23, 32]. The functional activities of respiratory chain complexes were studied by substrate-inhibitor titration [23, 33].

Mitochondrial contribution to the energy metabolism was measured in non-permeabilized cells. Following stabilization of endogenous routine respiration (ROUTINE) 2 µg/ml of oligomycin was added to inhibit ATP synthesis and induce the nonphosphorylating leak state (LEAK). Maximal uncoupled respiratory rates were determined with FCCP titration followed by inhibition of electron transfer by 10 µM antimycin A to measure residual oxygen consumption (ROX).

2.1.4 Metabolic control analysis (MCA)

In MCA, the degree of the control that a given enzyme exerts on the flux can be described quantitatively as a flux control coefficient (FCC). If the enzyme exerts an elevated control over the regulation of the metabolic pathway, then even a small change in the given enzyme activity will promote a significant variation in the pathway flux[34-35].

FCCs were determined for all mitochondrial ETC complexes, adenine nucleotide translocator (ANT) and inorganic phosphate carrier after their stepwise titration with specific pseudo irreversible inhibitors upon direct activation of respiration by exogenously added ADP (at 2 mM). The following inhibitors were used: rotenone for Complex-I of the mitochondrial electron transport chain (ETC); atpenin A5 for Complex-II; antimycin A for Complex-III; sodium cyanide for Complex-IV; oligomycin for complex-V (ATP synthase); carboxyatractyloside (CAT) for ANT; and mersalyl for inorganic phosphate carrier.

2.1.5 Assays of enzymes activity

The enzyme activities were studied spectrophotometrically at 25 °C using a Cary 100 Bio UV-visible spectrophotometer. The activity of HK was measured as the total glucose phosphorylating capacity of whole cell extracts, using a standard glucose-6-phosphate dehydrogenase (G6PDH)-coupled spectrophotometric assay [36]. The activity of CK was measured by a coupled enzyme assay in the presence of di(adenosine-5') pentaphosphate (adenylate kinase inhibitor[37]), 20 mM phosphocreatine (PCr) and with 2 U/ml G6PDH and 2 U/ml HK as the coupled enzymes[38].

The total AK activity was also measured by a coupled enzyme assay[39]. In order to determine the specific activities of AK1 and AK2, lysates were incubated with AK1 inhibitor N-ethylmaleimide(NEM) for 1h at 25°C. AK2 activity was determined as the activity remaining after the NEM treatment. AK1 activity was calculated as total AK activity minus activity remaining after the NEM treatment.

The activity of citrate synthase (CS) was measured by monitoring the production of CoA from oxaloacetate together with acetyl-CoA. The thiol group of CoA reacts with 5,5'-dithiobis-(2-nitrobenzoic acid) (Ellman's reagent, DTNB) to produce a yellow-colored product which was observed by measuring the absorbance at 412 nm. Reactions were performed in 96-well plates containing 100mM Tris-HCl pH 8.1, 0.3mM AcCoA, 0.5mM oxaloacetate and 0.1mM DTNB using FLUOstar Omega plate-reader spectrophotometer (BMG Labtech).

2.1.6 Confocal imaging

2102Ep cells were seeded on glass coverslips in 12-well plates (Greiner bio-one) and allowed to adhere overnight. H9 cells were passaged onto Matrigel coated glass coverslips and cultured in 12-well plates for 3 days. Then, the growth medium was removed and cells were incubated with 200nM MitoTracker Red CMXRos for 30 min at 37°C to stain mitochondria. After staining, cells were fixed in 4% paraformaldehyde in PBS during 15 min at RT. Following permeabilization with ice-cold methanol for 20min at RT, cells were incubated with 2% BSA in PBS for 1 h at RT, probed with specific primary antibodies against Oct-4 and incubated for 1h at RT. After incubation, cells were washed with PBS and incubated with corresponding fluorescence-conjugated secondary antibodies. Finally, cells were incubated for 15 min at RT with 4',6-diamidino-2-phenylindole dihydrochloride (DAPI, Molecular Probes™) to visualize the cell nucleus. Cells were imaged by an Olympus FluoView FV1000 inverted laser scanning confocal microscope.

2.1.7 Isolation of RNA, cDNA synthesis and qPCR

Total RNA from Ep2102 and hES cells was isolated using FavorPrep™ Blood/Cultured Cell Total RNA Mini Kit (Favorgen Biotech Corporation) and quantitated using a Nanodrop spectrophotometer (ND-1000; Nanodrop). Following DNaseI (Thermo Fisher Scientific) treatment, reverse transcription was performed on 1 µg of total RNA with random hexamer primers using RevertAid RT Reverse Transcription Kit (Thermo Fisher Scientific) according to the manufacturer protocol. The synthesized cDNA was subjected to quantitative PCR analysis using 5x HOT FIREPol® Probe Universal qPCR Mix (Solis BioDyne) and specific primers actin beta – Hs01060665_g1; hexokinase I – Hs00175976_m1; hexokinase II – Hs00606086_m1; creatine kinase brain-type HS00176484_m1; creatine kinase, mitochondrial 1B – Hs00179727_m1; creatine kinase, mitochondrial 2 – Hs00176502_m1, adenylate kinase 1 HS00176119_m1; adenylate kinase 2 HS01123132_g1; adenylate kinase 4 HS03405743_g1. All qPCR experiments were performed on LightCycler 480 II Real-Time PCR System (Roche) with following conditions: 95 °C for 10 min followed by 40 cycles of 95 °C for 15 sec and 60 °C for 1 min. PCR reactions were performed in triplicate for each of three independent experiments and included no reverse transcriptase and no template negative controls. Threshold cycles (Ct) were automatically calculated by LightCycler 480 software (Roche). Data were analyzed with the formula $2^{-\Delta\Delta C_t}$ (Livak and Schmittgen, 2001), normalized to the endogenous control ActB and expressed as fold change over hESC samples.

2.1.8 Statistical analysis of data

All data points are presented as means \pm standard error (SEM) from at least five separate experiments performed in duplicate. Significance was calculated by Student's t-test; differences between two data groups were considered to be statistically significant when $p < 0.05$.

3 Results

3.1 2102Ep cells displayed elevated levels of adenylate kinase 2 (AK2) and reduced levels of creatine kinase (CK) compared to hESCs

2102Ep demonstrated a distinct expression pattern of key enzymes that are involved in cellular energy homeostasis (Fig.1). The measurements of enzymatical activities further clarified the differences between hESC and 2102Ep cells. Compared to hESCs, the total creatine kinase activity was significantly decreased in 2102Ep cells (Table1) in accordance with the down-regulation of creatine kinase mitochondrial (CKMT1A) and brain (CKB) isoforms (Fig.1). Interestingly, both cell lines had very low expression of CKMT2 and the expression level of CKMT1A was significantly higher. This suggests CKMT1A to be the main isoform of mitochondrial CK expressed in these cells. Concomitantly, the total adenylate kinase activity was significantly increased in 2102Ep cells (Table 1) and was most probably associated with a nearly 2-fold higher expression level of AK2 isoform in 2102Ep cells than in hESC (Fig.1). Although the expression of AK1 was lower in 2102Ep cells (Fig.1), this was not reflected on its enzymatical activity (Table 1). We observed no statistical difference in the expression levels of AK4 between two cell lines (Fig.1).

3.2 The respiration is compromised in 2102Ep cells compared to hESCs

To characterize the ability of cells to consume oxygen we performed OCR studies. The intactness of mitochondrial outer and inner membranes was controlled by standard mitochondrial membrane integrity test (Fig.2A)[40]. The addition of cytochrome c (8 μ M) had no effect on oxygen consumption rate, while the addition of carboxyatractyloside (1 μ M) decreased the respiration rate to the basal level indicating the intactness of outer and inner mitochondrial membranes. In order to ensure the quality of the cells, this test was performed prior to every experiment.

State 2 (in the absence of ADP) and state 3 (in the presence of ADP) respiration rates were determined and compared between these two cell lines. State 3 respiration rate in 2102Ep cells was remarkably lower than in hESCs (5.04 ± 0.37 versus 7.45 ± 0.58 ,

$p=0.01$)(Fig.2B).Respiratory control ratios (RCRs) were calculated as the ratios between state 2 and state 3 respiration. Because of reduced state 3 respiration, RCR was two times lower in the 2102Ep cells (1.98 ± 0.10 versus 3.99 ± 0.36 , $p=0.005$) (Fig.2C).

3.3 Mitochondrial contribution to the energy metabolism of hESCs and 2102Ep cells

For the understanding of mitochondrial contribution to the energy metabolism of hESC and 2102Ep cell lines, we analyzed OCR response of these cells to the combination of inhibitors (oligomycin, antimycin) and uncoupler of OXPHOS (FCCP) (Fig.3A, B). After monitoring routine respiration, oligomycin, the inhibitor of ATP synthase, was added to uncouple the ATP-linked respiration from the proton leak. As shown in figure 3C, 50% of routine respiration (State 2 respiration measured without permeabilization of the cell membrane) was dedicated to ATP production. The proton leak appears to be very similar in these two cell lines, accounting approximately 25% of the cellular respiration rate, indicating that the suppressed respiration of 2102Ep cells is not due to the decreased proton leak. After addition of oligomycin, maximal respiratory rate was determined by FCCP treatment. FCCP is a protonophore that uncouples electron transport and mitochondrial respiration from ATP synthesis by dissipating the proton gradient. The addition of FCCP resulted in an increase of oxygen consumption levels in both cell lines with a more pronounced response in 2102Ep cells. The difference between oxygen consumption rate following FCCP treatment and State 2 respiration rate represents the respiratory capacity of these cells. We observed that the mitochondrial respiratory capacity was higher for 2102Ep cells when compared with hESCs (Fig.3C).The addition of mitochondrial Complex I and III inhibitors rotenone and antimycin reduced respiration rates in both cell lines, although this effect was significantly more pronounced in 2102Ep cells (Fig.3B).

3.4 2102Ep demonstrated stronger coupling between HK and OXPHOS than hESCs

To examine if reduced level of oxygen consumption is associated with increased level of glycolysis in 2102Ep cells, we compared the activity and expression levels of HK, an enzyme that catalyzes the first reaction of glycolysis, between these two cell lines. Although 2102Ep cells had a 2-fold decrease in HK2 mRNA level, the total HK activity was similar between studied cell lines (Fig.1, Table 1).

To evaluate the coupling between HK and OXPHOS, we investigated the effect of glucose on cellular respiration (Fig.4). It can be seen that addition of 0.1 mM ATP increased in the respiration rate due to the generation of a large flux of ADP from ATPases in hESCs. The effect of glucose on the oxygen consumption was characterized by glucose index (I_{glu}), which represents the degree of glucose-stimulated respiration compared to maximal ADP-stimulated respiration. The I_{glu} calculated for 2102Ep cells was considerably higher compared to hESCs, 55.16 ± 2.21 versus 40.18 ± 4.64 , respectively ($p=0.06$), suggesting that coupling between HK reactions and OXPHOS are more pronounced in 2102Ep cells (Fig.4B). These results suggest that 2102Ep cells prefer more aerobic glycolysis to produce ATP than hESC.

3.5 hESCs and 2102Ep have a functional mitochondrial respiratory chain

In order to identify mechanisms of mitochondrial respiratory chain that could account for the lower oxygen consumption rate in 2102Ep, we examined the functional activity of respiratory chain complexes I-IV and ATP-synthase in both cell types. Our data demonstrated that all complexes within the mitochondrial respiratory chain of hESCs and 2102Ep cells were functionally active and their activities were equivalent in both cell lines (Fig.5). Firstly, ADP stimulated respiration was blocked by rotenone (20 μ M, Complex I inhibitor), restored by addition of succinate (10 mM, Complex II substrate) and then, inhibited again by antimycin A (10 μ M, Complex III inhibitor), indicating the functional activity of Complexes I, II and III. Finally, the functional activity of Complex IV was confirmed by the addition of electron donors ascorbic acid (5mM) and N,N,N',N'-tetramethyl-p-phenylenediamine(TMPD, 1 mM), which strongly enhanced oxygen consumption in both cell types (Fig.5).

The morphological features of hESC and 2102Ep cells were examined by confocal microscopy (Fig.6). Although both cell lines expressed pluripotency marker Oct-4 and contained some spontaneously differentiated cells, there were several differences in cell morphology. While hESCs grow as colonies and display high nucleus to cytoplasm ratio, 2102Ep cells grow as a monolayer and contain considerably larger volumes of cytoplasm. Consistent with previous reports[9], hESCs display punctuate mitochondria with predominantly perinuclear localization, whereas in 2102Ep cells mitochondria localize randomly in the cytoplasm (Fig.6). To ensure that alterations in mitochondrial respiration rates were not due to differences in mitochondrial content, the CS activity assay was performed. Our results (Table 1) indicated a similar mitochondrial mass in both cell lines.

3.6 Metabolic control analysis revealed the differences of regulation of cellular respiration in 2102Ep and hESCs

To further analyze mitochondrial respiration in hESCs and 2102Ep cells, the sensitivity of mitochondrial respiratory chain complexes to specific inhibitors was measured and the degree of control that each individual complex exerts on whole respiration chain was evaluated using MCA method[41]. Flux control coefficients (FCC) for mitochondrial complexes I-IV, ATP-synthase, adenine nucleotide translocator (ANT) and phosphor carrier (Pi) are summarized in Table 2. Our results showed that the key sites for the regulation of respiration are Complex I (FCC=0.76), and Complex IV (FCC=1.02) in hESCs. In 2102Ep cells, Complex II (FCC=0.75) and Complex IV (FCC=1.24) are the main regulators, since FCC values for other complexes were considerably lower (Table 2). It was impossible to determine FCC for Complex III in hESCs, because of the high sensitivity of these cells to Complex III inhibition. Beyond 0.15 nM of antimycin A, the inhibition was suddenly increased and the rate of respiration dropped sharply.

Our results indicated a notable difference in the control exerted by the phosphorylating system of OXPHOS constituted by the ATP synthase, ANT and Pi carrier in 2102Ep and hESCs. The FCC for ANT in 2102Ep cells exceeded 8 times the value obtained for hESCs (FCC=0.62 versus FCC=0.07). On the contrary, the FCC for Pi carrier was significantly lower in 2102Ep cells (FCC=0.03 versus FCC=0.26). The FCC value estimated for ATP synthase was 3 times higher in 2102Ep cells (FCC=0.63) compared to hESCs (FCC=0.22).

The total FCCs values for both cell types exceeded significantly the theoretic value for linear systems, which is considered to be close to 1[42]. 2102Ep cells had higher total FCC values (FCC=3.98) than hESCs (FCC>2.7). Altogether, these results demonstrate that the role of respiratory chain complexes and ATP synthase in energy metabolism of 2102Ep cells differ considerably from that in normal stem cells.

4 Discussion

Cancer stem cells may acquire numerous properties of normal stem cells including their ability to self-renew, relative quiescence, expression of the same surface markers and activation of the same cell signaling pathways [43]. The specific depletion of CSC that represents a promising approach in clinical cancer therapy is challenging due to this similarity. Therefore, it is necessary to discover cellular or metabolic features that could help to distinguish CSCs from normal stem cells. In order to elucidate the possible differences, we

have chosen normal hESC (H9) to compare with embryonal carcinoma cells (2102Ep) that express similar pluripotency-associated marker proteins but have limited differentiation ability[44].

In normal cells, the oxidative phosphorylation is closely linked to phosphotransfer systems where adenylate kinase and creatine kinase networks transport ATP from mitochondria to ATP-consumption sites[16]. We have demonstrated that the expression and the activity of several major components of the phosphotransfer system vary notably between 2102Ep cells and hESCs. In the current study, the deficiency of CK network was accompanied by the up-regulation of AK network in 2102Ep cells. The significant decrease of CK levels has been previously reported upon the transformation of skeletal muscle into sarcoma [45]. Several reports have indicated reduced levels of CK in brain cancer, colon cancer, prostate cancer and other malignancies [20, 46]. The current findings about the expression and activity of different AK isoforms during cancerogenesis are contradictory. Although the increased expression of AK2 has been found in breast CSC[47] and prostate cancer cells[48], another study states that AK2 is rather a negative regulator of tumor growth[49]. On the other hand, it has been reported that the up-regulation of AK2 provides the energy required for the proliferation of hematopoietic stem cells [50] and plays an important role in communication between mitochondria and nucleus [16]. AK2 deficiency impairs embryonic development and causes hematopoietic defects indicating the significance of AK2 in the energy metabolism of normal stem cells [50-51]. Further studies are needed to find out how AK2 expression and its compartmentalization influence cellular proliferation. A brief analysis of data from The Cancer Genome Atlas (TCGA) using the cBioPortal shows genomic alterations (amplification, deletion, or base pair mutation) in phosphotransfer systems in many cancers (Fig. 1S). The most frequent alteration was detected in breast cancer xenografts where 48% of tumors exhibited amplified number of AK2 and HK2 suggesting that tumor cells with elevated levels of AK2 and HK2 may be one of the key players in cancer development and progression. A closer look at specific AK2 and HK2 alterations across various tumors reveals that amplification is the most common genomic alteration of AK2 while HK2 might be either amplified or mutated (Table 1S).

In agreement with previous reports, our results demonstrated that both normal and cancer stem cells have functional mitochondria. Although CSCs are often considered to be a glycolytic cell type, many recent reports identify oxidative metabolism as the preferred energy production mechanism in various CSCs [17, 52]. Moreover, it has been shown that functional

mitochondria are crucial for the maintenance of CSC phenotype [17, 47]. Enhanced mitochondrial function of CSCs has been associated with tumor growth [53], increased metastatic potential [54] and resistance to chemotherapy [55].

Our results showed that 2102Ep cells consume lower levels of oxygen than normal stem cells. The reduced respiration rate may indicate that the mitochondrial respiratory chain does not operate sufficiently to generate an effective proton gradient. However, our results demonstrated that reduced mitochondrial respiration in 2102Ep cells was not the result of the impairment of respiratory chain complexes because all mitochondrial respiratory complexes were functionally active and their activities were equivalent in both cell lines. No differences were found between the rates of proton leak in studied cell lines. Mitochondria are functioning in the vast majority of cells at a basal energy level that is required for cell survival and normal performance. The term “reserve respiratory capacity” is used to characterize the additional capacity available in cells to produce energy in response to certain conditions or increased stress [56]. One possible reason for the elevated reserve respiratory capacity in 2102Ep cells could be the increase of substrate entry into the TCA cycle [57]. In support of this hypothesis, it has been shown that TCA cycle intermediates are enriched in another (NTERA2) human embryonal carcinoma cell line [58].

We applied MCA to identify target reactions that control respiratory chain activity in 2102Ep cells and hESCs. Our results from MCA provided indirect evidence to conclude that the complexes II and IV share larger control strength over respiration in 2102Ep than in hESCs. Complex I exerted larger control over respiration in hESCs. Interestingly, Complex I has been shown to play an important role in cellular differentiation by generating reactive oxygen species (ROS) that stimulate muscle cell differentiation [59]. Taking into account that 2102Ep cells exhibit reduced ability to differentiate; Complex I in these cells may have distinct functional features compared to hESCs.

Completely different control patterns were also obtained for ATP synthase and its associated substrate suppliers, Pi carrier, and ANT. It has long been known that the coupling of ATP synthesis to oxygen consumption is not perfect due to the proton leak across the inner membrane of mitochondria [60]. Two groups of mitochondrial proteins contribute significantly to proton leak, uncoupling proteins and the adenine nucleotide translocator [61]. In current work the FCC for ANT was considerably higher in 2102Ep cells, showing that ANT exerts a higher degree of control over respiration and may play an important role in the

regulation of proton leak in these cells. This is supported by the recent finding that the regulation of mitochondrial proton leak depends on the metabolic conditions.[62]. Thus, it can be assumed that the regulation of proton leak could be also distinctly mediated in cells with different cellular metabolic states. However, additional research is needed to control this hypothesis.

The total FCCs were higher than expected for both hESCs and 2102Ep cells, contradicting the summation theorem of MCA according to which the sum of the FCCs of the enzymes of a metabolic pathway should be equal to 1. High total FCCs in both cell lines might be the result of branched pathways or direct substrate channeling between the protein (super)complexes [42]. Very little is known about the organization of respiratory chain in stem cells. It has been shown that the differentiation of human mesenchymal stem cells (hMSCs) is accompanied by the increased mitochondrial biogenesis and formation of supercomplexes[8, 63]. *Hoffmann et al.* has confirmed the presence of several supercomplexes in hMSCs, although the number of supramolecular assemblies was significantly reduced compared with differentiated cells[8]. It has been shown that in mitochondria with impaired respiration, ATP synthase and ANT may operate in the opposite direction compared with normal cells generating high ATP level and reverse proton gradient[64]. Definitely, the role of mitochondrial biogenesis and OXPHOS organization in the regulation of cellular differentiation and cancer development represents an important direction for future research.

Rapidly proliferating hESCs and CSCs are forced to adapt their cellular metabolism to meet their demand for energy and increased biosynthesis of macromolecules[65]. The Warburg effect represents one of the most common adaptive mechanisms which is acquired by highly proliferative and malignant cells to support their metabolic needs [66]. While the majority of normal differentiated cells use glycolysis followed by aerobic oxidation of pyruvate in the mitochondria to eventually produce ATP, highly proliferating cells prefer glycolysis followed by lactic acid fermentation during the process called “aerobic glycolysis” or “Warburg effect”[66]. Although aerobic glycolysis provides less ATP per molecule of glucose, it produces energy much faster and provides many intermediates for the production of proteins, lipids, and nucleotides[67]. In order to compare the level of aerobic glycolysis in our experimental models (Warburg-Pedersen) we evaluated the effect of exogenously added glucose on the cellular respiration. Our results showed up-regulation of aerobic glycolysis in 2102Ep compared to hESCs.

Altogether, our results confirm that the embryonal carcinoma 2102Ep cells display distinct bioenergetic profile compared to normal hESCs. The shift in energy distribution towards AK network, alterations in the regulation of respiratory chain as well as suppressed respiration may serve as indicators of tumorigenic stem cell. In addition, as differences in bioenergetic profile indicate different regulation of various cellular processes, this data should be taken into account for future use of these cell lines as *in vitro* stem cell or cancer stem cell models. Clearly, further extensive characterization of bioenergetics of normal and cancer cells is necessary in order to extend our knowledge of the mechanisms behind the cellular proliferation and differentiation. Ultimately, this will help to develop an effective treatment that would selectively target CSCs sparing normal stem cells and, thus, reducing side effects of conventional anti-cancer therapy.

5 Conclusions

Current study shed light on several aspects of energy metabolism in normal and tumorigenic stem cells. Our results showed that the bioenergetic profile of 2102Ep cells clearly distinguishes them from normal hESCs. Reduced oxygen consumption, increased aerobic glycolysis and shifted energy metabolism towards AK network represented the bioenergetic signature of this carcinoma cell line. Present and future studies will potentially aid in the understanding of metabolic properties of stem cells and establishment of effective strategies for identifying cells with increased tumorigenic potential.

Acknowledgements

The authors are thankful to Annika Trei for culturing the hESC.

Funding

The work of LO, AK, KT, NT, VC, IS and TK was supported by institutional research funding IUT23-1 of the Estonian Research Council. The work of MP, IT and TM was supported by a grant PUT0374 from the Estonian Research Council. This work of NP, KP and SK was supported by institutional research funding IUT20-46 of the Estonian Research Council.

FIGURE LEGENDS

Fig.1. Comparison of the mRNA expression levels of key enzymes involved in cellular energy homeostasis in hESCs and 2102Ep cells. Expression of the indicated mRNA was

quantified using qPCR. Data were normalized to β -actin mRNA and expressed as a fold change relative to hESCs. The results are means \pm SEM of three individual studies. * $p < 0.05$ and ** $p < 0.005$

Fig.2. Respiratory properties of hESC and 2102Ep cells.(A) Mitochondrial membranes integrity validation test. Adenosine diphosphate, ADP; Cytochrome c, Cyt c; Carboxyatractyloside, CAT. (B) State 2 and state 3 respiration rates. All rates were normalized to total protein concentration in the same samples. (C) Respiratory control indexes (RCIs). RCIs were calculated as the ratios between state 2 and state 3 rates. All data are mean \pm SEM of 5–6 independent experiments. * $p < 0.05$.

Fig.3. Assessment of mitochondrial function in hESCs and 2102Ep cells.(A) Representative respirometric trace with schematic representation of the mitochondrial function assay. Arrows indicate the titrations into the oxygraph chamber. Maximal respiratory rate was determined with FCCP titration. Maximal uncoupled respiration was reached at $0.5\mu\text{M}$ FCCP followed by inhibition of electron transfer (ETS) by antimycin A to measure residual oxygen consumption (ROX). (B) Quantitative analysis of mitochondrial OCR readings. (C) Functional properties of mitochondrial respiration. Proton leak was calculated as $(V_{\text{LEAK}} - V_{\text{ROX}}) / V_{\text{ROUTINE}}$; ATP-linked respiration: $(V_{\text{ROUTINE}} - V_{\text{LEAK}}) / V_{\text{ROUTINE}}$; maximal respiration: $(V_{\text{FCCP}} - V_{\text{ROX}}) / V_{\text{ROUTINE}}$; respiratory reserve capacity: $(V_{\text{FCCP}} - V_{\text{ROUTINE}}) / V_{\text{ROUTINE}}$.

Fig.4.Effect of exogenously added glucose on the rate of oxygen consumption. The effect of glucose was estimated as a degree of glucose-mediated respiration compared to State 3 respiration and expressed as the glucose index (I_{glu}): $I_{\text{glu}}(\%) = (V_{\text{glu}} - V_{\text{ATP}}) / (V_{\text{ADP}} - V_{\text{ATP}})$. Results represent means \pm SEM, $n=5$. The difference in the mean values of the two groups is statistically significant, * $p < 0.05$. Cytochrome c, Cyt c.

Fig.5.Functional activity of respiratory chain complexes. The Complex IV-dependent respiration was calculated as $V_{\text{TMPD}/\text{Asc}} - V_{\text{TMPD}/\text{Asc}+\text{NaCN}}$ where $V_{\text{TMPD}/\text{Asc}}$ and $V_{\text{TMPD}+\text{NaCN}}$ are TMPD-stimulated respiration rates before and after addition of NaCN. Results represent means \pm SEM, $n=5$. Asc – ascorbate, TMPD - N,N,N',N'-tetramethyl-p-phenylenediamine, CI, CII, CIII and CIV – Complexes I, II, III and IV respectively. Bars are SEM.

Fig.6. Immunocytochemical analysis of Oct-4 (green) and MitoTracker Red (red) in hESC and 2102Ep cells. Nuclei are stained with DAPI (blue). Scale bars, $10\mu\text{m}$.

TABLES**Table 1.** The activity of HK, CK and CS in hESCs and 2102Ep cells

	Enzyme activities, mU/mg protein		<i>p</i> -values
	hESC mean±SEM	2102Ep mean±SEM	
Hexokinase	67.28±2.75	71.46±7.91	0.64
Creatine kinase	159.84±3.70	12.75±2.15	<0.0001
Citrate synthase	52.26±3.07	64.77±4.26	0.08
Total adenylate kinase (AK)	64.39±2.55	179.85±5.73	<0.001
AK1	28.77±1.6 (46%*)	37.44±3.86 (21%)	0.1
AK2	33.10±1.00 (54%)	142.42±3.29 (79%)	<0.001

Notes: *% from the total AK activity.

Table 2. Flux control coefficients (FCC) of respiratory chain complexes for hESCs and 2102Ep cells

ETC component	Inhibitor	hESCs, FCC	2102Ep, FCC
Complex I	Rotenone	0.76	0.40
Complex II	Atpenin A5	0.37	0.75
Complex III	Antimycin A	NA	0.31
Complex IV	Na cyanide	1.02	1.24
ATP synthase	Oligomycin	0.22	0.63
ANT	Carboxyatractyloside	0.07	0.62
Pi carrier	Mersalyl	0.26	0.03

References

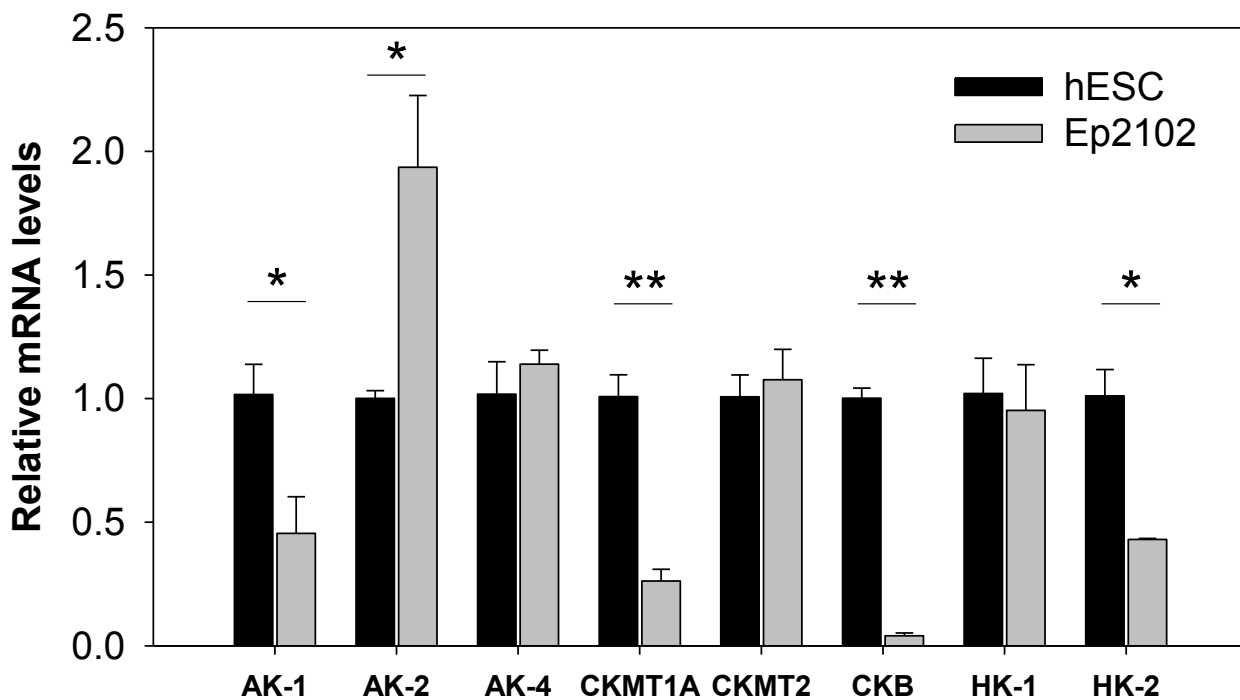
1. Adams, P.D., H. Jasper, and K.L. Rudolph, *Aging-Induced Stem Cell Mutations as Drivers for Disease and Cancer*. Cell Stem Cell, 2015. **16**(6): p. 601-12.
2. Clarke, M.F., et al., *Cancer stem cells--perspectives on current status and future directions: AACR Workshop on cancer stem cells*. Cancer Res, 2006. **66**(19): p. 9339-44.
3. Fanali, C., et al., *Cancer stem cells in colorectal cancer from pathogenesis to therapy: controversies and perspectives*. World journal of gastroenterology, 2014. **20**: p. 923-42.
4. Dragu, D.L., et al., *Therapies targeting cancer stem cells: Current trends and future challenges*. World journal of stem cells, 2015. **7**: p. 1185-201.
5. Vidal, S.J., et al., *Targeting cancer stem cells to suppress acquired chemotherapy resistance*. Oncogene, 2014. **33**: p. 4451-63.
6. Shackleton, M., *Normal stem cells and cancer stem cells: similar and different*. Seminars in cancer biology, 2010. **20**: p. 85-92.
7. Han, S., et al., *Mitochondrial biogenesis and energy production in differentiating murine stem cells: a functional metabolic study*. Cellular reprogramming, 2014. **16**: p. 84-90.
8. Hofmann, A.D., et al., *OXPHOS supercomplexes as a hallmark of the mitochondrial phenotype of adipogenic differentiated human MSCs*. PLoS One, 2012. **7**(4): p. e35160.
9. Vega-Naredo, I., et al., *Mitochondrial metabolism directs stemness and differentiation in P19 embryonal carcinoma stem cells*. Cell death and differentiation, 2014. **21**: p. 1560-74.
10. Varum, S., et al., *Enhancement of human embryonic stem cell pluripotency through inhibition of the mitochondrial respiratory chain*. Stem cell research, 2009. **3**: p. 142-56.
11. Zhang, J., et al., *UCP2 regulates energy metabolism and differentiation potential of human pluripotent stem cells*. The EMBO journal, 2011. **30**: p. 4860-73.
12. Hanahan, D. and Robert A. Weinberg, *Hallmarks of Cancer: The Next Generation*. Cell, 2011. **144**: p. 646-674.
13. Warburg, O., *On respiratory impairment in cancer cells*. Science, 1956. **124**(3215): p. 269-70.
14. Hu, C., et al., *Energy Metabolism Plays a Critical Role in Stem Cell Maintenance and Differentiation*. International journal of molecular sciences, 2016. **17**.
15. Pedersen, P.L., *Warburg, me and Hexokinase 2: Multiple discoveries of key molecular events underlying one of cancers' most common phenotypes, the "Warburg Effect", i.e., elevated glycolysis in the presence of oxygen*. Journal of bioenergetics and biomembranes, 2007. **39**: p. 211-22.
16. Dzeja, P.P. and A. Terzic, *Phosphotransfer networks and cellular energetics*. The Journal of experimental biology, 2003. **206**: p. 2039-47.

17. Janiszewska, M., et al., *Imp2 controls oxidative phosphorylation and is crucial for preserving glioblastoma cancer stem cells*. Genes & development, 2012. **26**: p. 1926-44.
18. Chung, S., et al., *Developmental restructuring of the creatine kinase system integrates mitochondrial energetics with stem cell cardiogenesis*. Annals of the New York Academy of Sciences, 2008. **1147**: p. 254-63.
19. Dzeja, P.P., et al., *Developmental enhancement of adenylate kinase-AMPK metabolic signaling axis supports stem cell cardiac differentiation*. PloS one, 2011. **6**: p. e19300.
20. Pan, H., et al., *Low serum creatine kinase levels in breast cancer patients: a case-control study*. PLoS One, 2013. **8**(4): p. e62112.
21. Bera, S., et al., *Enzymes of creatine biosynthesis, arginine and methionine metabolism in normal and malignant cells*. The FEBS journal, 2008. **275**: p. 5899-909.
22. Klepinin, A., et al., *Comparative analysis of some aspects of mitochondrial metabolism in differentiated and undifferentiated neuroblastoma cells*. Journal of Bioenergetics and Biomembranes, 2014. **46**: p. 17-31.
23. Chekulayev, V., et al., *Metabolic remodeling in human colorectal cancer and surrounding tissues: alterations in regulation of mitochondrial respiration and metabolic fluxes*. Biochemistry and Biophysics Reports, 2015. **4**: p. 111-125.
24. Amamoto, R., et al., *The Expression of Ubiquitous Mitochondrial Creatine Kinase Is Downregulated as Prostate Cancer Progression*. Journal of Cancer, 2016. **7**: p. 50-9.
25. Andrews, P.W., et al., *Cell-surface antigens of a clonal human embryonal carcinoma cell line: morphological and antigenic differentiation in culture*. Int J Cancer, 1982. **29**(5): p. 523-31.
26. Josephson, R., et al., *Qualification of Embryonal Carcinoma 2102Ep As a Reference for Human Embryonic Stem Cell Research*. Stem Cells, 2007. **25**: p. 437-446.
27. Hovatta, O., et al., *A Teratocarcinoma-Like Human Embryonic Stem Cell (hESC) Line and Four hESC Lines Reveal Potentially Oncogenic Genomic Changes*. PLoS ONE, 2010. **5**: p. e10263.
28. Ben-Porath, I., et al., *An embryonic stem cell-like gene expression signature in poorly differentiated aggressive human tumors*. Nat Genet, 2008. **40**(5): p. 499-507.
29. Wong, D.J., et al., *Module map of stem cell genes guides creation of epithelial cancer stem cells*. Cell Stem Cell, 2008. **2**(4): p. 333-44.
30. Andrews, P.W., et al., *Embryonic stem (ES) cells and embryonal carcinoma (EC) cells: opposite sides of the same coin*. Biochem Soc Trans, 2005. **33**(Pt 6): p. 1526-30.
31. Andrews, P.W., *Human embryonal carcinoma cells in culture do not synthesize fibronectin until they differentiate*. Int J Cancer, 1982. **30**(5): p. 567-71.
32. Eimre, M., et al., *Distinct organization of energy metabolism in HL-1 cardiac cell line and cardiomyocytes*. Biochim Biophys Acta, 2008. **1777**(6): p. 514-24.

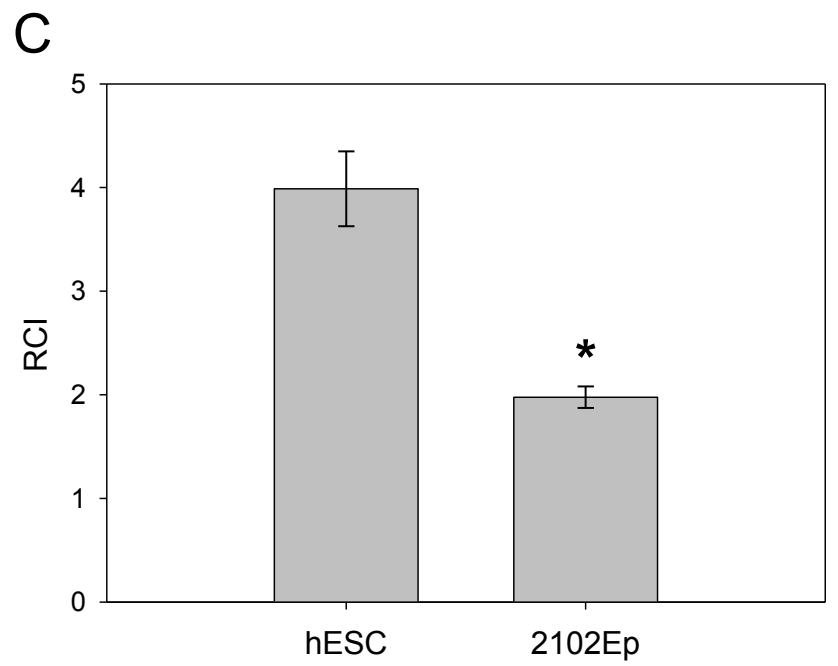
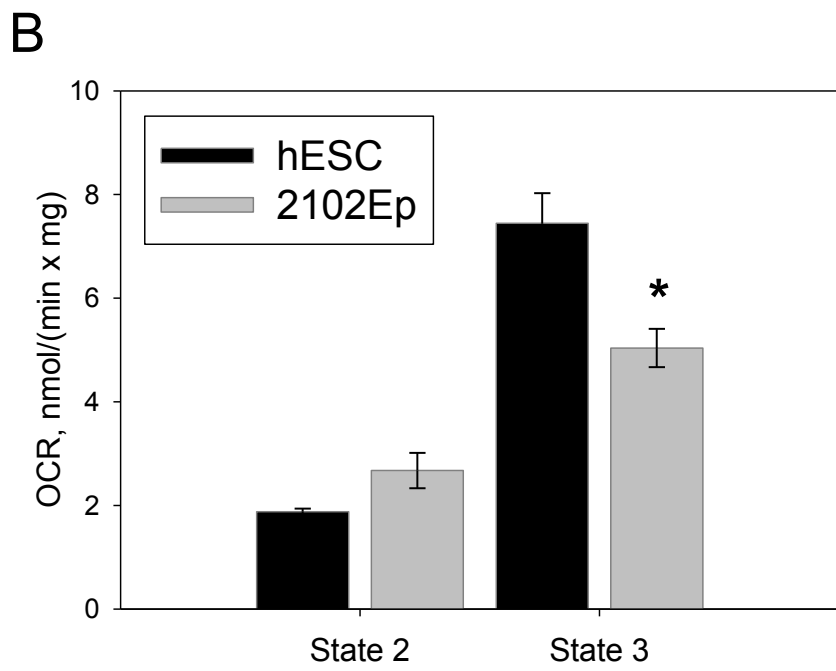
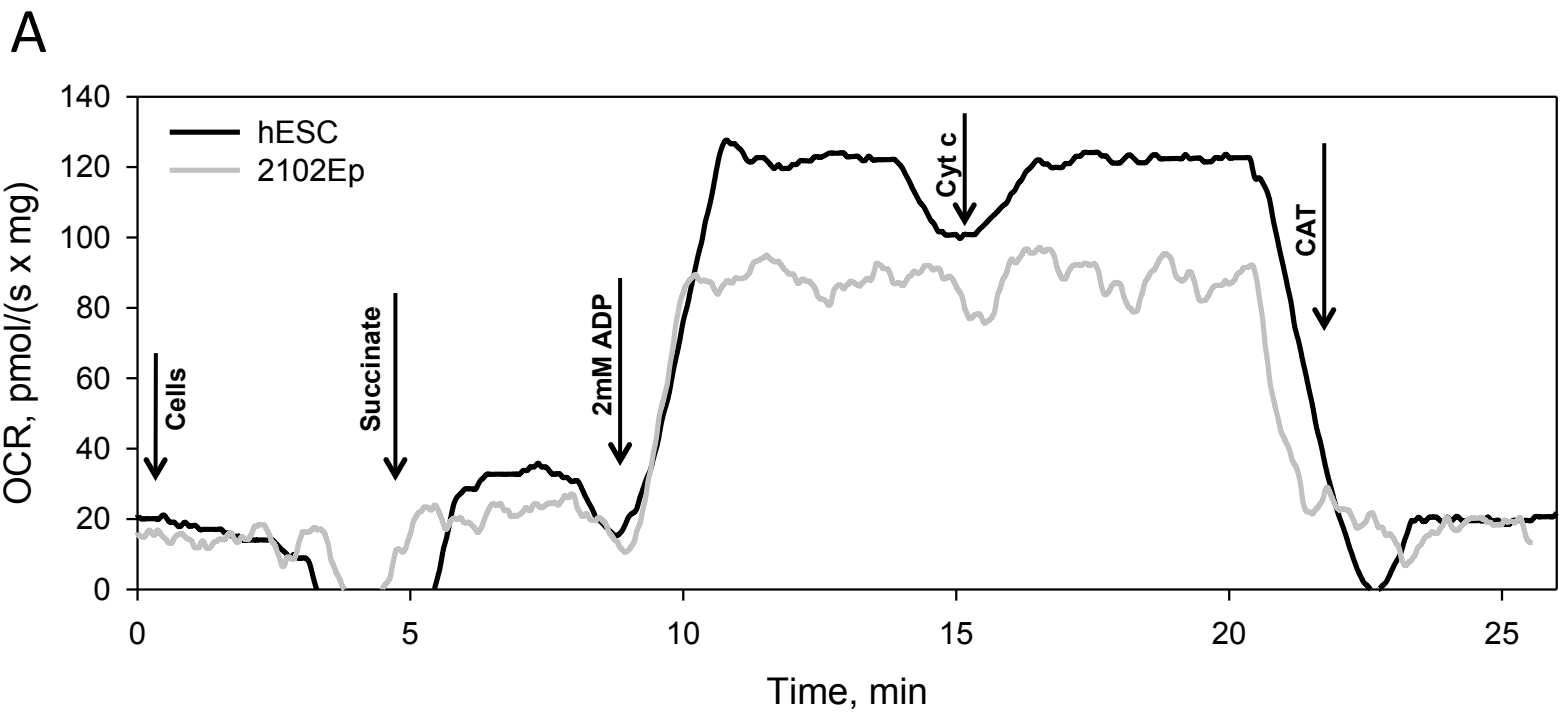
33. Puurand, M., et al., *Deficiency of the complex I of the mitochondrial respiratory chain but improved adenylate control over succinate-dependent respiration are human gastric cancer-specific phenomena*. Mol Cell Biochem, 2012. **370**(1-2): p. 69-78.
34. Fell, D., *Understanding the control of metabolism*. Frontiers in metabolism 2, ed. K. Snell. 1997, London , Miami: Portland Press. xii, 301 p.
35. Tepp, K., et al., *Metabolic control analysis of integrated energy metabolism in permeabilized cardiomyocytes - experimental study*. Acta biochimica Polonica, 2010. **57**: p. 421-30.
36. Biswas, S., et al., *Selective inhibition of mitochondrial respiration and glycolysis in human leukaemic leucocytes by methylglyoxal*. The Biochemical journal, 1997: p. 343-8.
37. Lienhard, G.E. and I.I. Secemski, *P 1 ,P 5 -Di(adenosine-5')pentaphosphate, a potent multisubstrate inhibitor of adenylate kinase*. The Journal of biological chemistry, 1973. **248**: p. 1121-3.
38. Monge, C., et al., *Comparative analysis of the bioenergetics of adult cardiomyocytes and nonbeating HL-1 cells: respiratory chain activities, glycolytic enzyme profiles, and metabolic fluxes*. Canadian journal of physiology and pharmacology, 2009. **87**: p. 318-26.
39. Dzeja, P.P., et al., *Adenylate kinase-catalyzed phosphotransfer in the myocardium : increased contribution in heart failure*. Circulation research, 1999. **84**: p. 1137-43.
40. Pesta, D. and E. Gnaiger, *High-resolution respirometry: OXPHOS protocols for human cells and permeabilized fibers from small biopsies of human muscle*. Methods Mol Biol, 2012. **810**: p. 25-58.
41. Moreno-Sanchez, R., et al., *Metabolic control analysis: a tool for designing strategies to manipulate metabolic pathways*. J Biomed Biotechnol, 2008. **2008**: p. 597913.
42. Kholodenko, B.N., O.V. Demin, and H.V. Westerhoff, *'Channelled' pathways can be more sensitive to specific regulatory signals*. FEBS Lett, 1993. **320**(1): p. 75-8.
43. Reya, T., et al., *Stem cells, cancer, and cancer stem cells*. Nature, 2001. **414**: p. 105-111.
44. Matthaei, K.I., P.W. Andrews, and D.L. Bronson, *Retinoic acid fails to induce differentiation in human teratocarcinoma cell lines that express high levels of a cellular receptor protein*. Exp Cell Res, 1983. **143**(2): p. 471-4.
45. Patra, S., et al., *Progressive decrease of phosphocreatine, creatine and creatine kinase in skeletal muscle upon transformation to sarcoma*. The FEBS journal, 2008. **275**: p. 3236-47.
46. Joseph, J., A. Cardesa, and J. Carreras, *Creatine kinase activity and isoenzymes in lung, colon and liver carcinomas*. British journal of cancer, 1997. **76**: p. 600-5.
47. Lamb, R., et al., *Mitochondrial mass, a new metabolic biomarker for stem-like cancer cells: Understanding WNT/FGF-driven anabolic signaling*. Oncotarget, 2015. **6**: p. 30453-71.
48. Hail, M., et al., *Adenylate Kinase: An Oncodevelopmental Marker in an Animal Model for Human Prostatic Cancer*. CLIN. CHEM. CLINICAL CHEMISTRY, 1985. **3110**: p. 1689-1691.

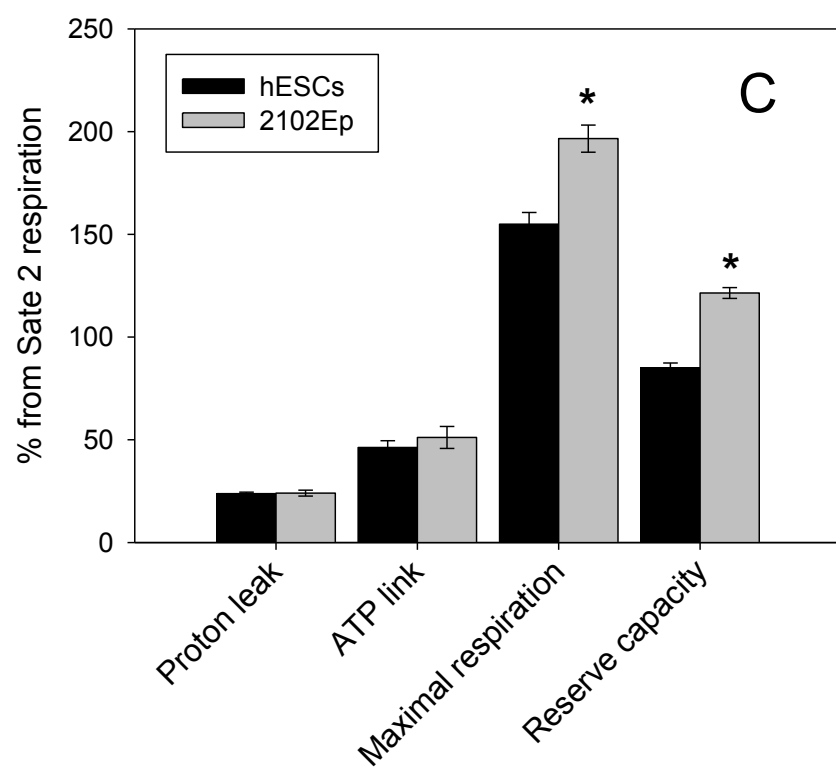
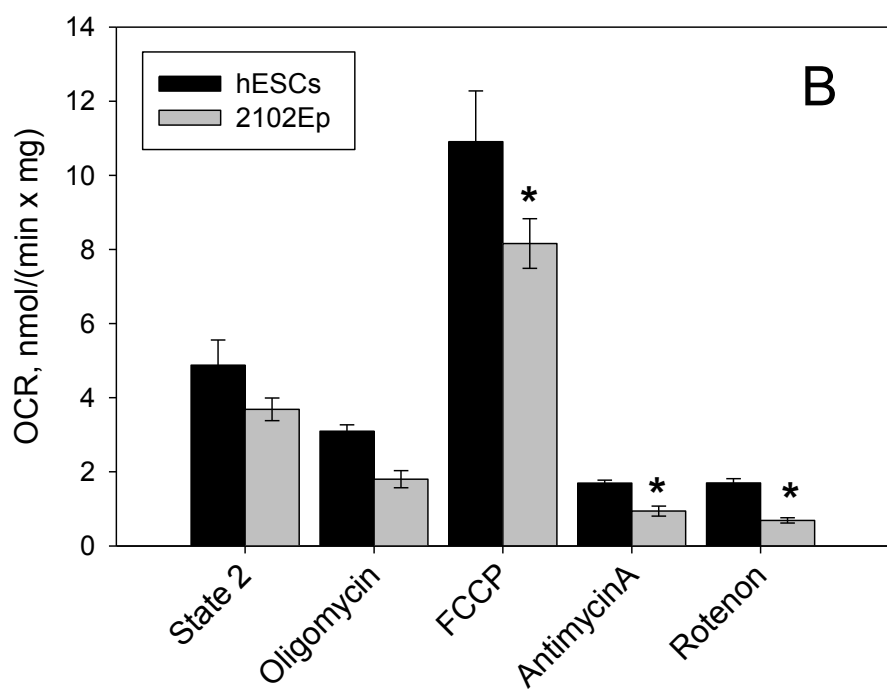
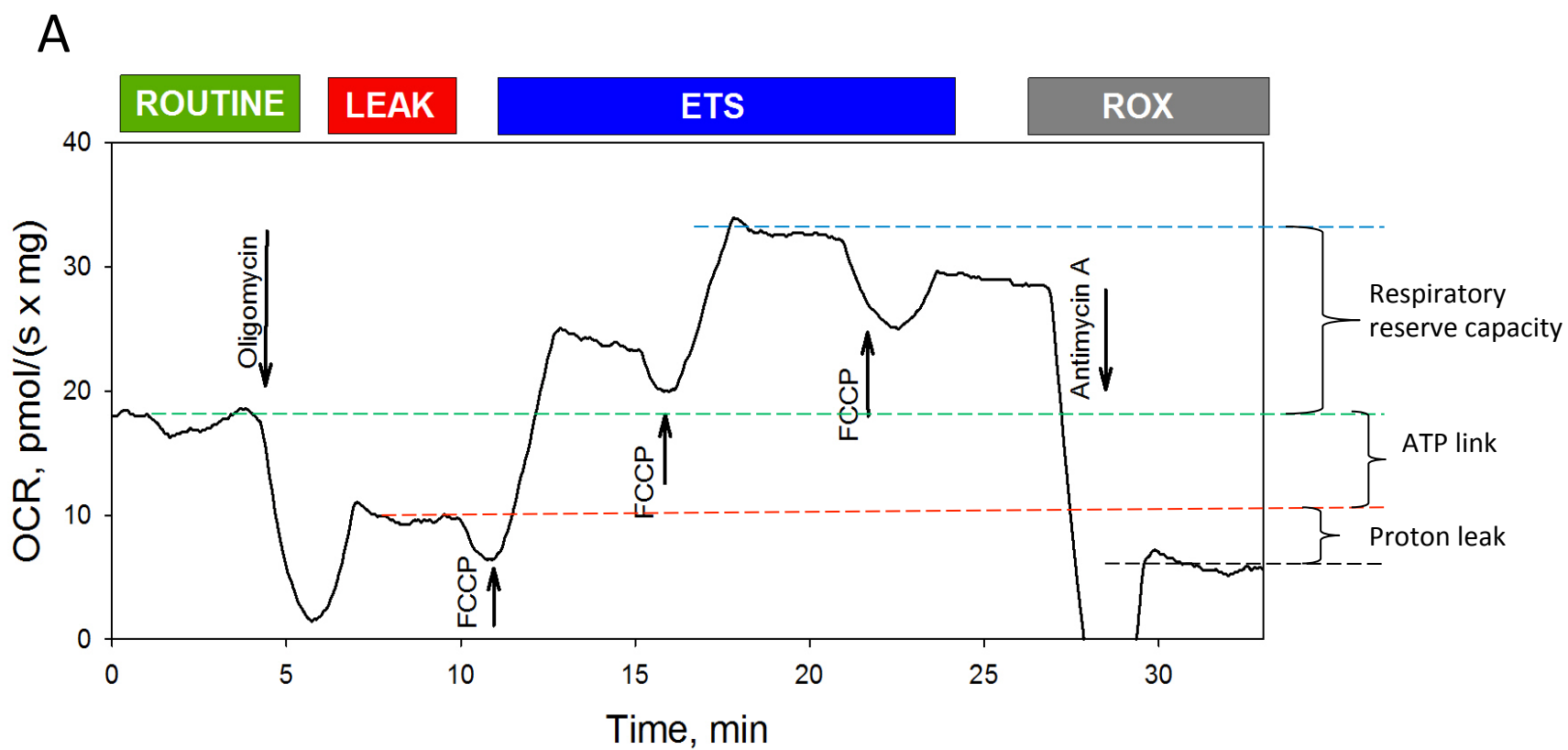
49. Kim, H., et al., *The DUSP26 phosphatase activator adenylate kinase 2 regulates FADD phosphorylation and cell growth*. Nature communications, 2014. **5**: p. 3351.
50. Lagresle-Peyrou, C., et al., *Human adenylate kinase 2 deficiency causes a profound hematopoietic defect associated with sensorineural deafness*. Nature genetics, 2009. **41**: p. 106-11.
51. Fujisawa, K., et al., *Adenylate kinase isozyme 2 is essential for growth and development of Drosophila melanogaster*. Comparative biochemistry and physiology. Part B, Biochemistry & molecular biology, 2009. **153**: p. 29-38.
52. Pastò, A., et al., *Cancer stem cells from epithelial ovarian cancer patients privilege oxidative phosphorylation, and resist glucose deprivation*. Oncotarget, 2014. **5**: p. 4305-19.
53. Salem, A.F., et al., *Mitochondrial biogenesis in epithelial cancer cells promotes breast cancer tumor growth and confers autophagy resistance*. Cell cycle (Georgetown, Tex.), 2012. **11**: p. 4174-80.
54. LeBleu, V.S., et al., *PGC-1 α mediates mitochondrial biogenesis and oxidative phosphorylation in cancer cells to promote metastasis*. Nature cell biology, 2014. **16**: p. 992-1003, 1-15.
55. Farnie, G., F. Sotgia, and M.P. Lisanti, *High mitochondrial mass identifies a sub-population of stem-like cancer cells that are chemo-resistant*. Oncotarget, 2015. **6**: p. 30472-86.
56. Desler, C., et al., *Is There a Link between Mitochondrial Reserve Respiratory Capacity and Aging?* J Aging Res, 2012. **2012**: p. 192503.
57. Pflieger, J., M. He, and M. Abdellatif, *Mitochondrial complex II is a source of the reserve respiratory capacity that is regulated by metabolic sensors and promotes cell survival*. Cell Death Dis, 2015. **6**: p. e1835.
58. Abu Dawud, R., et al., *Human embryonic stem cells and embryonal carcinoma cells have overlapping and distinct metabolic signatures*. PLoS One, 2012. **7**(6): p. e39896.
59. Lee, S., et al., *Mitochondrial H₂O₂ generated from electron transport chain complex I stimulates muscle differentiation*. Cell Res, 2011. **21**(5): p. 817-34.
60. Stuart, J.A., et al., *Mitochondrial proton leak and the uncoupling proteins*. Journal of bioenergetics and biomembranes, 1999. **31**: p. 517-25.
61. Jastroch, M., et al., *Mitochondrial proton and electron leaks*. Essays in biochemistry, 2010. **47**: p. 53-67.
62. Cardoso, S., et al., *UCP2 and ANT differently modulate proton-leak in brain mitochondria of long-term hyperglycemic and recurrent hypoglycemic rats*. Journal of Bioenergetics and Biomembranes, 2013. **45**: p. 397-407.
63. Chen, C.T., et al., *Coordinated changes of mitochondrial biogenesis and antioxidant enzymes during osteogenic differentiation of human mesenchymal stem cells*. Stem Cells, 2008. **26**(4): p. 960-8.
64. Chevrollier, A., et al., *Adenine nucleotide translocase 2 is a key mitochondrial protein in cancer metabolism*. Biochim Biophys Acta, 2011. **1807**(6): p. 562-7.

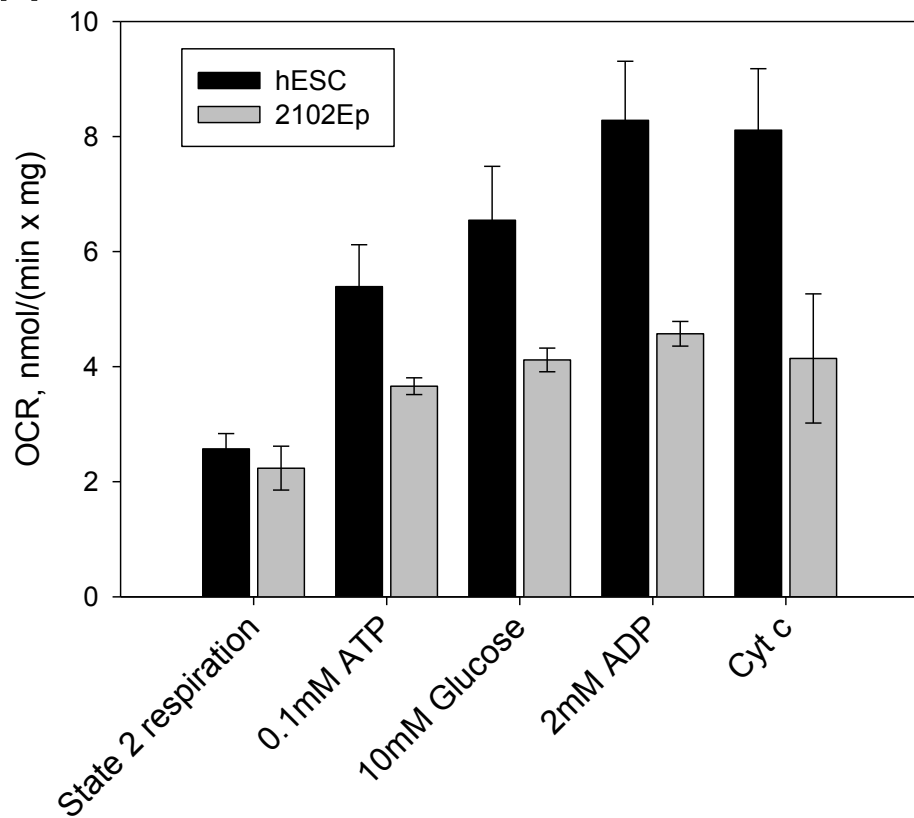
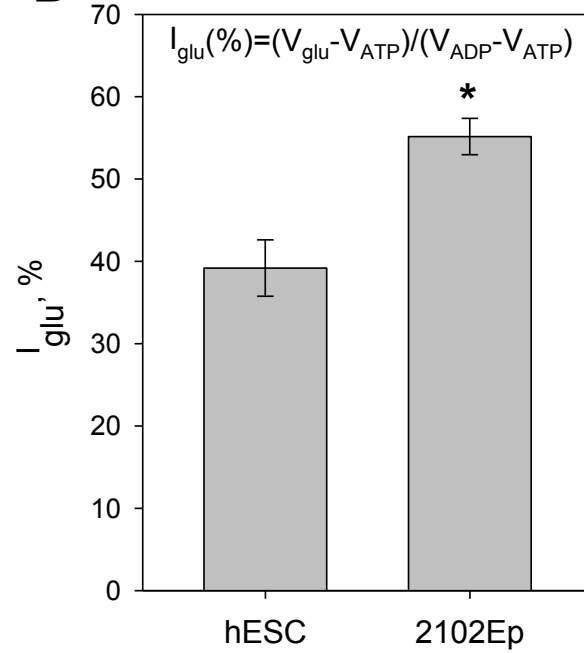
65. Jang, H., et al., *Metabolism in embryonic and cancer stemness*. Archives of Pharmacal Research, 2015. **38**: p. 381-388.
66. Gaspar, J.A., et al., *Unique Metabolic Features of Stem Cells, Cardiomyocytes, and Their Progenitors*. Circulation Research, 2014. **114**: p. 1346-1360.
67. Lunt, S.Y. and M.G. Vander Heiden, *Aerobic glycolysis: meeting the metabolic requirements of cell proliferation*. Annual review of cell and developmental biology, 2011. **27**: p. 441-64.

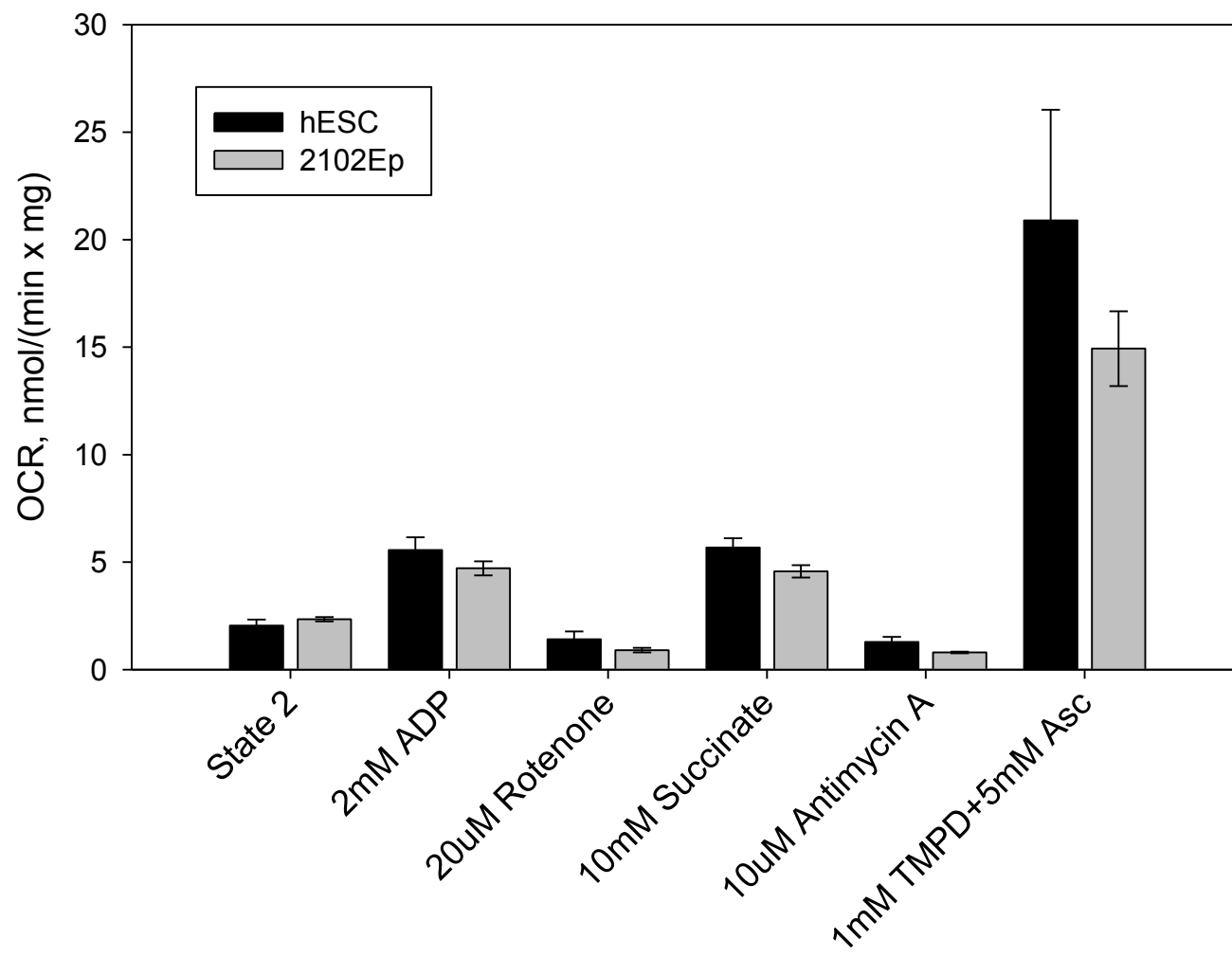


\\fs2\BEL\experiments\stem cells\Ep2102_paper_figures

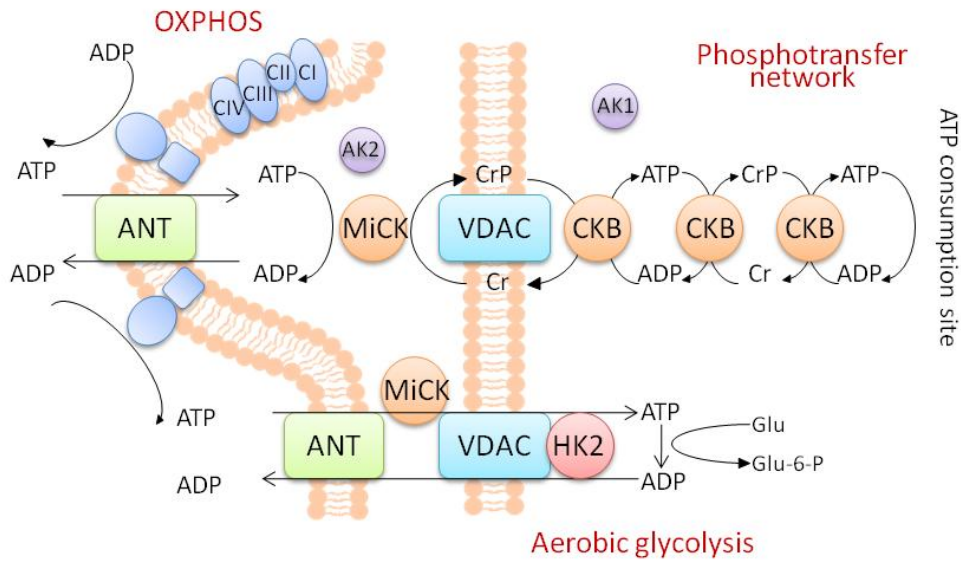




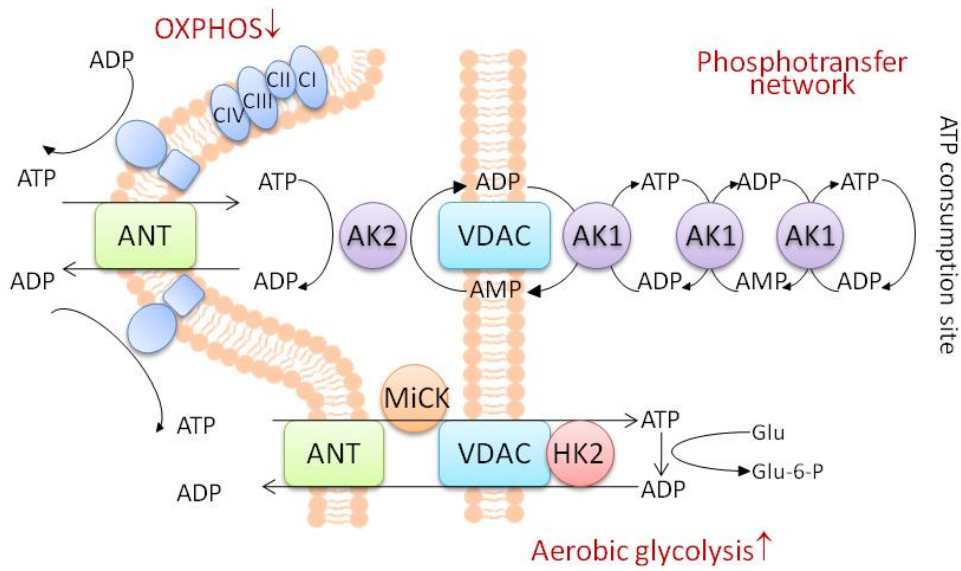
A**B**



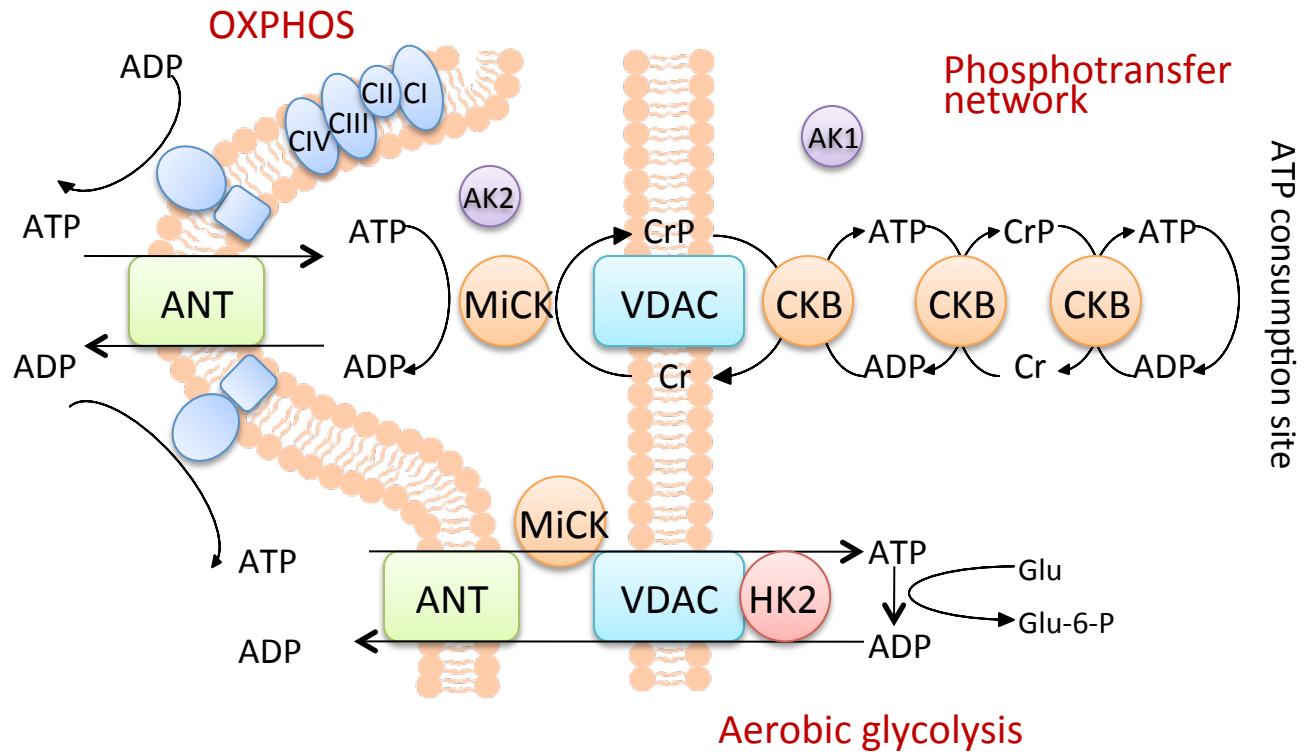
Normal stem cells (H9)



Carcinoma stem cells (2102Ep)



Normal stem cells



Carcinoma stem cells

